Title

Simulating biogenic volatile organic compound emissions in the Community Climate System Model

Journal

Journal of Geophysical Research, 108(D21)

ISSN

0148-0227

Authors

Levis, Samuel

Wiedinmyer, Christine

Bonan, Gordon B

et al.

Publication Date

2003-11-16

DOI

10.1029/2002jd003203

Simulating biogenic volatile organic compound emissions in the Community Climate System Model

Samuel Levis, Christine Wiedinmyer, Gordon B. Bonan, and Alex Guenther
National Center for Atmospheric Research, Boulder, Colorado, USA

Received 21 November 2002; revised 30 May 2003; accepted 14 August 2003; published 4 November 2003.

[1] The Community Climate System Model (CCSM) calculates terrestrial biogenic volatile organic compound (BVOC) emissions using an algorithm developed from field and laboratory observations. This algorithm is incorporated in CCSM, a coupled atmosphere, ocean, sea ice, and land model, as one step toward integrating biogeochemical processes in this model. CCSM is designed to easily incorporate more complex BVOC models in the present framework when such models become available. Two simulations are performed: a land-only simulation driven with prescribed atmospheric data and satellite-derived vegetation data and a fully coupled CCSM simulation with prognostic vegetation using CCSM's dynamic vegetation model. In both cases, warm and forested regions emit more BVOC than other regions, in agreement with observations. With prescribed vegetation, global terrestrial isoprene emissions of 507 Tg C per year compare well with other model simulations. With dynamic vegetation, BVOC emissions respond to varying climate and vegetation from year to year. The interannual variability of the simulated biogenic emissions can exceed 10% of the estimated annual anthropogenic emissions provided in the IPCC emission scenarios. We include BVOC emissions within the CCSM to ultimately reduce the simulated climate uncertainty due to natural processes in this model. *INDEX TERMS:* 0315 Atmospheric Composition and Structure: Biosphere/atmosphere interactions; 0345 Atmospheric Composition and Structure: Pollution—urban and regional (0305); 1615 Global Change: Biogeochemical processes (4805); 3322 Meteorology and Atmospheric Dynamics: Land/atmosphere interactions; *KEYWORDS:* biogeochemistry, CCSM, VOC

Citation: Levis, S., C. Wiedinmyer, G. B. Bonan, and A. Guenther, Simulating biogenic volatile organic compound emissions in the Community Climate System Model, *J. Geophys. Res.*, *108*(D21), 4659, doi:10.1029/2002JD003203, 2003.

1. Introduction

[2] Vegetation contributes about 90% of the nonmethane Volatile Organic Compounds (VOC) emitted globally to the atmosphere [*Guenther et al.*, 1995]. These biogenically emitted VOC (hereafter BVOC) include isoprene (C_5H_8), monoterpenes ($C_{10}H_{16}$), and other reactive carbon compounds. The amount of carbon in global BVOC emissions may exceed 1 Pg yr^{-1} [*Guenther et al.*, 1995].

[3] Many BVOC react with ozone and other oxidants in the atmosphere, with effects on local, regional, and global atmospheric chemistry [*Fehsenfeld et al.*, 1992; *Houweling et al.*, 1998]. For example, *Poisson et al.* [2000] simulated a 15% increase in the tropospheric lifetime of methane due to the presence of BVOC. Secondary organic aerosol formation from BVOC emissions is estimated to range from 13–24 Tg yr^{-1} [*Griffin et al.*, 1999] to 30–270 Tg yr^{-1} [*Andreae and Crutzen*, 1997]. This amount of aerosol is similar in magnitude to the estimates of carbonaceous aerosol emitted globally to the atmosphere from fossil fuel and biomass combustion [*Liousse et al.*, 1996]. Aerosols affect the atmosphere's radiative balance directly by scattering and absorbing light, and indirectly when they act as cloud condensation nuclei [e.g., *Penner et al.*, 2001].

[4] Through their effects on atmospheric chemistry, aerosol concentrations, and the global carbon cycle, BVOC emissions potentially influence global climate [*Constable et al.*, 1999]. *Collins et al.* [2002] show that isoprene has a positive secondary global warming potential. The Intergovernmental Panel on Climate Change (IPCC) includes nonmethane VOC emissions in their recommended emission scenarios for climate models. These scenarios estimate about 140 Tg C yr^{-1} of VOC from anthropogenic sources for the mid-1990s, and from less than 100 to more than 550 Tg C yr^{-1} for 2100 [*Nakicenovic et al.*, 2000].

[5] BVOC emissions vary by plant species and depend on environmental conditions such as temperature, solar radiation, plant water stress, and ambient ozone and carbon dioxide concentrations [e.g., *Penuelas and Llusia*, 2001]. Algorithms have been developed from field and laboratory research to simulate BVOC emissions [e.g., *Guenther et al.*, 1995] to show, for example, that a 6 K rise in annual temperature may double isoprene emissions in a Texas savanna [*Guenther et al.*, 1999]. These models require land cover and meteorological data as inputs. Past studies have simulated point, regional, and global emissions successfully [e.g., *Guenther et al.*, 1995; *Pierce et al.*, 1998; *Guenther et*

0148-0227/03/2002JD003203

Table 1. A Summary of Differences Between the Offline Approach of Including BVOC Emissions in Atmospheric Models and the Present Approach, Which is Online or Synchronously Coupled[a]

Approach	INPUT DATA	Use of the Output
Offline emissions (past work): Externally derived input data → BVOC emission model → atmospheric transport and chemistry model	1. LAI: satellite-derived OR empirically calculated offline from climate-plant productivity relationships 2. vegetation types and cover: many classes for fine distinction in emission capacities 3. temperature: observed or simulated offline by atmospheric model 4. radiation: as with temperature but, sometimes, run through an offline canopy radiative transfer model to calculate attenuation and the direct and diffuse components of the radiation	BVOC emissions prescribed as input to atmospheric transport and chemistry model; one-way interaction
Online emissions in climate system model (this study): Model-derived inputs → BVOC emission model embedded in land surface model → atmospheric transport and chemistry model embedded in climate model Simplifies the introduction of new algorithms that use existing land model processes (e.g., soil moisture and plant water stress)	1. LAI: satellite-derived or dynamically simulated 2. vegetation types and cover: satellite-derived; fewer types but can easily lengthen the list 3. temperature: simulated by climate model 4. radiation: simulated by climate model; online canopy radiative transfer model calculates attenuation and direct and diffuse components of the radiation	BVOC emissions instantly passed to atmospheric transport and chemistry model that operates within the climate model; synchronous coupling allows for two-way interactions between atmospheric transport, chemistry, climate, and vegetation

[a]In the current implementation of the online approach the atmosphere model does not yet include a transport and chemistry model.

al., 2000]. To further track BVOC concentrations and their chemical transformations, BVOC emission rates are input into atmospheric transport and chemistry models [e.g., *Poisson et al.*, 2000; *Bouchet et al.*, 1999]. The results from such models have been used to examine BVOC chemistry and to investigate BVOC effects on regional pollution [e.g., *Pierce et al.*, 1998].

[6] As an alternative to the iterative coupling of land-based emissions to atmosphere-based transport and chemistry, we use an integrated framework in which BVOC emissions are calculated within a land surface and dynamic vegetation model (Table 1). This model simulates ecological and physiological processes, which influence BVOC emissions, and operates as a component of a climate system model, including atmosphere, ocean, and sea ice components. The atmosphere component may include models of atmospheric chemistry and transport. This way, BVOC emissions, transport, and chemistry occur synchronously in an internally consistent framework. Synchronous coupling of processes is a favored approach when nonlinear interactions are involved and becomes imperative when surface characteristics change, as is the case with vegetation dynamics [*Foley et al.*, 2000].

[7] With this study, we evaluate our model's global scale BVOC emissions. We also assess the simulated interannual variability of these emissions. Ultimately, including BVOC emissions within a climate system model serves the purpose of reducing climate uncertainty from natural processes.

2. Methods

[8] We have incorporated the BVOC emission model developed by *Guenther et al.* [1995] into the Community Land Model version 2.0 (CLM) [*Bonan et al.*, 2002a]. The former is an emissions model developed from field and laboratory observations. The latter is a state of the art land surface model, which computes all the variables required by the BVOC model.

2.1. Community Land Model

[9] The Community Land Model version 2.0 (CLM) [*Bonan et al.*, 2002a] is a component of the Community Climate System Model version 2.0 (CCSM) [*Blackmon et al.*, 2001]. CCSM couples atmosphere, ocean, sea ice, and land processes synchronously in an internally consistent framework.

[10] The land component, CLM, simulates the exchange of water, carbon, energy, and momentum between land surfaces and the atmosphere through a wide range of ground and canopy biogeophysical processes. Vegetation is described in terms of plant functional types that arise from landscape differences observable from satellite (i.e., annual versus perennial vegetation, evergreen versus deciduous, and needleleaf versus broadleaf) [*Running et al.*, 1995]. These remotely sensed differences are further categorized into broad climatic groups (Table 2). CLM has a standard set of input data for the land surface (i.e., percent lake, wetland, glacier, and plant cover, as well as monthly leaf area index (LAI) per plant functional type). The land surface data are satellite-derived and are described in detail by *Bonan et al.* [2002b].

[11] As an alternative to using prescribed vegetation from satellite data, CLM can simulate global vegetation characteristics with the inclusion of a dynamic vegetation model [*Bonan et al.*, 2003; *Sitch et al.*, 2003]. In this case, plant biomass responds to climate variations from year to year; plant phenology (evergreen, summer green, rain green) responds to temperature and moisture conditions to determine daily LAI; and plant photosynthesis and respiration are calculated at every 20-min time step of the land model. The annually summed carbon balance influences the success of each plant functional type against its competitors in a model grid cell. *Bonan et al.* [2003] found the vegetation

Table 2. Emission Capacity for Isoprene, Monoterpenes, OVOC, ORVOC and CO for Each Plant Functional Type in CLM[a]

Plant Functional Type	Emission Capacity, μg C g^{-1} dry foliar mass h^{-1}					SLA, m^2 g^{-1} dry foliar mass
	Isoprene	Monoterpenes	OVOC	ORVOC	CO	
Needleleaf evergreen tree, temperate	2	2	1	1	0.3	0.00625
Needleleaf evergreen tree, boreal	4	2	1	1	0.3	0.00625
Needleleaf deciduous tree	0	1.6	1	1	0.3	0.00625
Broadleaf evergreen tree, tropical	24	0.4	1	1	0.3	0.01250
Broadleaf evergreen tree, temperate	24	0.8	1	1	0.3	0.01250
Broadleaf deciduous tree, tropical	24	0.8	1	1	0.3	0.01250
Broadleaf deciduous tree, temperate	24	0.8	1	1	0.3	0.01250
Broadleaf deciduous tree, boreal	24	0.8	1	1	0.3	0.01250
Broadleaf evergreen shrub, temperate	24	0.8	1	1	0.3	0.01250
Broadleaf deciduous shrub, temperate	24	0.8	1	1	0.3	0.01250
Broadleaf deciduous shrub, boreal	24	0.8	1	1	0.3	0.01250
C3 grass, arctic	0	0.1	1	1	0.3	0.01000
C3 grass	0	0.1	1	1	0.3	0.01000
C4 grass	0	0.1	1	1	0.3	0.01000
Crop	0	0.1	1	1	0.3	0.01000

[a]Also given are specific leaf area (SLA) values for each plant functional type from *Kucharik et al.* [2000].

dynamics simulated by this land model satisfactory for use with the fully coupled CCSM.

2.2. Module of BVOC Emissions

[12] Terrestrial BVOC fluxes are estimated from

$$F = \varepsilon D\, C_L\, C_T \quad (1)$$

[*Guenther et al.*, 1995], where F is the BVOC flux (μg C m^{-2} h^{-1}), ε (Table 2) is the plant type dependent emission capacity (μg C g^{-1} dry foliar mass h^{-1}) normalized to a photosynthetically active radiation (PAR) flux of 1000 μmol m^{-2} s^{-1} and a leaf temperature of 303.15 K, D is the foliar density (g dry foliar mass m^{-2}), and C_L and C_T are dimensionless empirical terms that modulate the emissions in response to incident PAR (isoprene only) and leaf temperature, respectively [*Guenther et al.*, 1993]. We calculate foliar density, D, by dividing LAI by the specific leaf area (Table 2). C_L is calculated separately for sunlit and shaded leaves with the assumption that only sunlit leaves receive direct-beam PAR, while sunlit and shaded leaves share the diffuse PAR as described by *Bonan* [1996].

[13] Emission factors have been measured for a wide variety of plant genera and species, which CLM does not represent explicitly. CLM employs the concept of plant functional type to describe vegetation in broad terms, for use within global climate and dynamic vegetation models. CLM's plant functional types are grouped into six emission factor categories (Table 2). Grasses and crops (four functional types) are assumed to have negligible isoprene emissions and very low monoterpene emissions as recommended by *Guenther et al.* [2000]. Needleleaf deciduous trees (1 type) are assigned the emission rates recommended for *Larix* species by *Guenther et al.* [1994]. Needleleaf evergreen trees tend to have high monoterpene emissions [*Guenther et al.*, 1994]. We have assigned relatively low isoprene emission factors to all needleleaf evergreen trees but have a higher factor for boreal (1 type) than temperate (one type) trees to account for the higher proportion of isoprene-emitting spruce trees in North American boreal forests. Tropical broadleaf evergreen trees (one type) are assigned the emission factors recommended by *Guenther et al.* [1995] for tropical rain forests. The remaining broadleaf trees and all shrubs (seven types) are assigned the global average rates suggested by *Guenther et al.* [1995]. This model does not account for BVOC fluxes from soils, which are lower than fluxes from vegetation by at least one order of magnitude.

2.3. Model Simulations

[14] We show results from two simulations here. (1) The first is a CLM simulation with prescribed NCEP atmospheric data for 1990 [*Kalnay et al.*, 1996] and prescribed satellite-derived vegetation (all data described in detail by *Bonan et al.* [2002b]). The model is run on a 1° in latitude by 1° in longitude grid for one model year. With this simulation we evaluate the model's ability to calculate BVOC emissions. Interannual variability would be negligible in this configuration, because incoming solar radiation and leaf area index vary seasonally in our data sets but not interannually. (2) The second is a present-day, T31 Gaussian grid (~3.75° in latitude by ~3.75° in longitude) CCSM simulation in which vegetation characteristics are simulated by CLM's vegetation dynamics. With this simulation we explore the potential for interannual variability in the simulated BVOC emissions as climate and vegetation evolve through time. This 150-year fully coupled simulation starts with spun up vegetation from a 400-year CLM simulation similar to (1) but with dynamic vegetation (initialized from bare ground). We consider CCSM's climate and vegetation to be near equilibrium, even though both continue to change due to model variability at a wide range of spatial and temporal scales. Global vegetation patterns agree with the observed except in parts of the boreal forest of Siberia and the temperate forest in eastern North America. In both cases tree cover is underestimated. The dynamic vegetation model simulates natural vegetation only. Human land use is omitted. The currently available atmospheric component of the CCSM does not include chemistry and transport of chemical species. We look at output from the final ten years of the 150-year simulation.

[15] In both simulations, isoprene, monoterpene, other reactive VOC (ORVOC), other VOC (OVOC), and carbon monoxide (CO) emissions are predicted at each 20-min time step. We discuss isoprene and monoterpene emissions, as

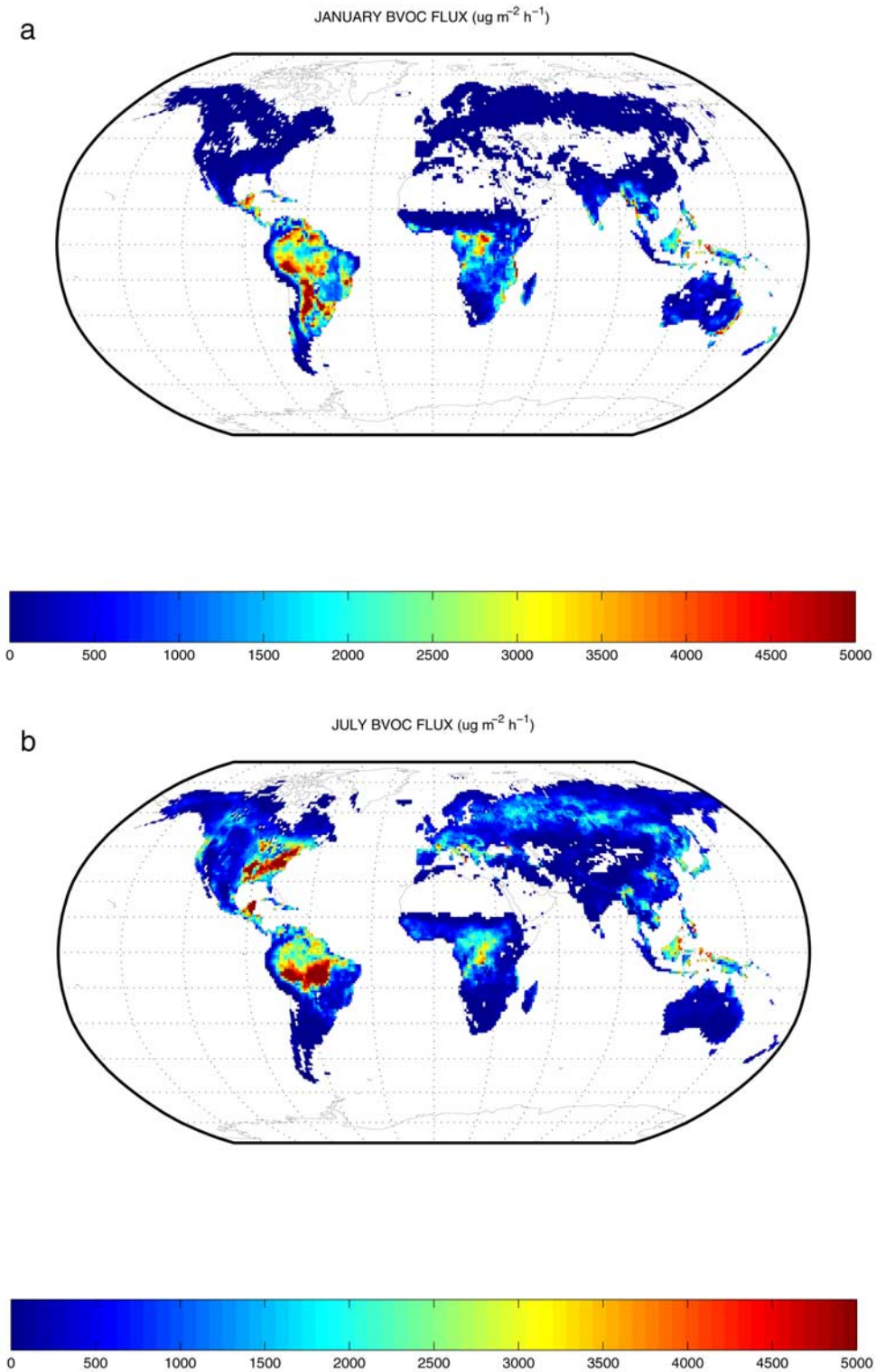

Figure 1. Terrestrial biogenic volatile organic compound (BVOC) emissions (a) for January and (b) for July. Zero is shown white. For comparison with isoprene observations in section 3.1, consider simulated isoprene emissions to be approximately two thirds of total BVOC.

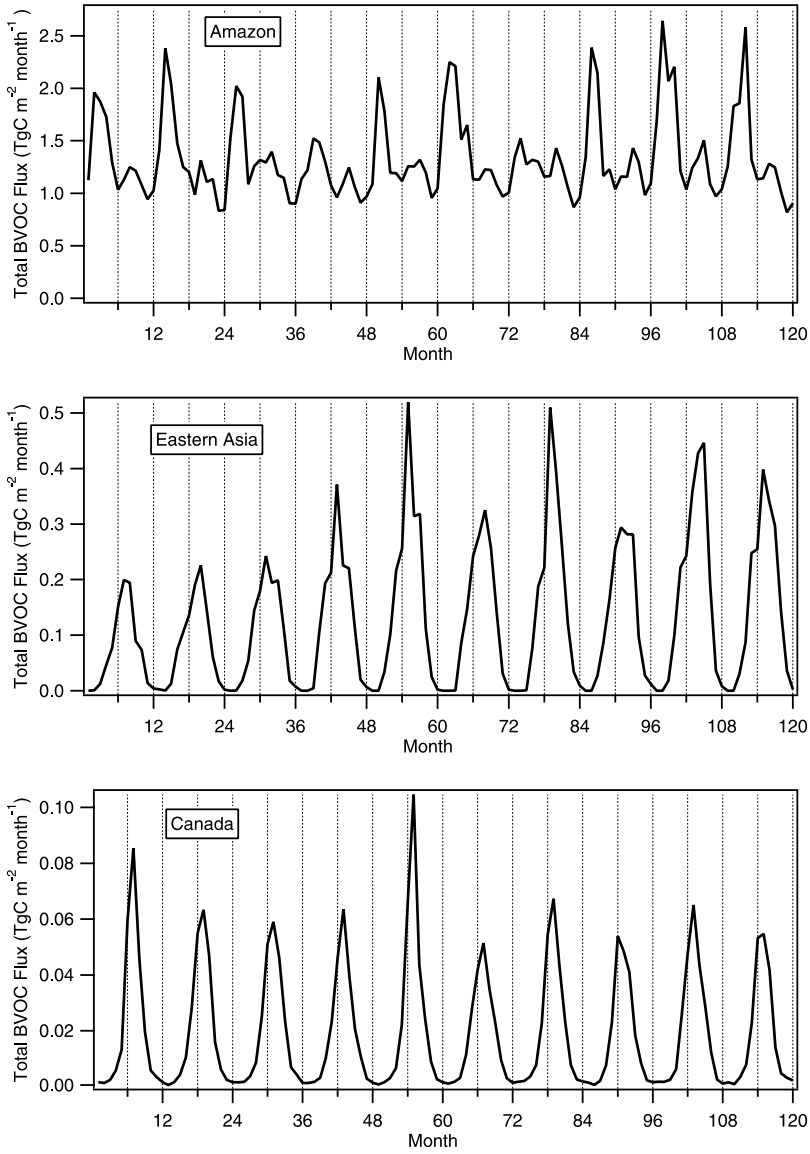

Figure 2. Monthly total BVOC emissions simulated at three grid cells: Amazon (tropical forest), eastern Asia (deciduous forest), and Canada (boreal forest).

well as total emissions from the sum of all five compound categories.

3. Results and Discussion

3.1. CLM Simulation

[16] Simulated BVOC emission patterns for January and July (Figure 1) agree with the global patterns simulated by *Guenther et al.* [1995]. Higher emissions occur where LAI, PAR, and temperature are higher. The tropics stand out as a source year-round, with some variability due to the annual LAI cycle of drought-deciduous trees. The extra-tropics respond to the annual LAI, PAR, and temperature cycles with higher emissions in summer and lower emissions in winter. Local maxima correspond to forests as opposed to deserts, grasslands, and crops. Certain regional maxima can also be attributed to the dominant plant functional type's emission capacity, ε. Broadleaf trees are assigned higher ε for isoprene than needleleaf trees, resulting in the particularly high summer emissions in the eastern half of the United States. Agreement with *Guenther et al.* [1995] suggests a satisfactory simulation of BVOC emissions by CLM.

[17] CLM simulates a global land BVOC emission of 692 Tg C annually, while *Guenther et al.* [1995] simulate 1145. Of the 692 Tg C, 507 are isoprene emissions and 33 are monoterpene emissions in CLM. *Guenther et al.* [1995] report these numbers as 503 and 127 Tg C. *Potter et al.* [2001], *Wang and Shallcross* [2000], and *Naik et al.* [2002], whose methodologies resemble ours in this simulation, quote 559, 530, and 456 Tg C of isoprene in their respective models. *Naik et al.* [2002] simulate 72 Tg C of monoterpene emissions.

[18] CLM's lower estimates compared to *Guenther et al.* [1995] for compounds other than isoprene are partly due to the use of lower emission capacities for certain plant types and partly due to differences in the land cover and LAI data sets. CLM's LAI values are generally lower than those used by *Guenther et al.* [1995]. BVOC emissions are directly

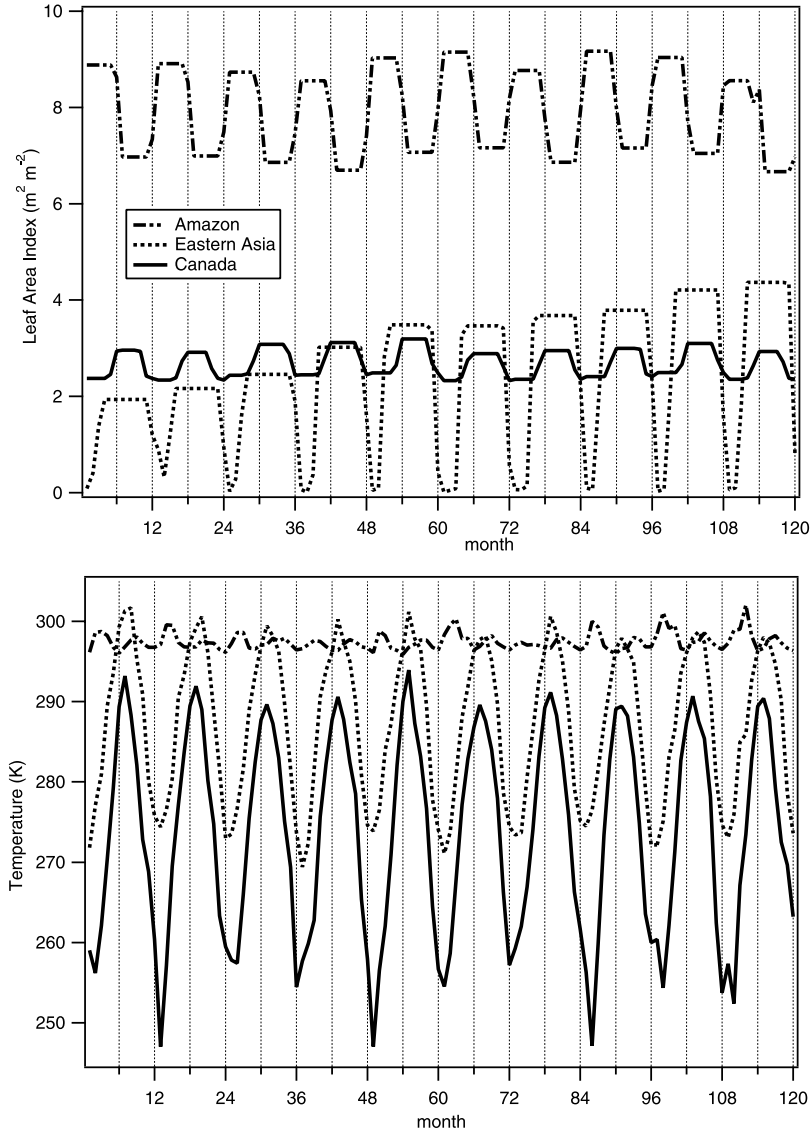

Figure 3. Simulated monthly LAI and leaf temperature at the three grid cells illustrated in Figure 2.

proportional to the LAI (equation (1)). We believe that CLM's vegetation and LAI data, derived entirely from satellite products [*Bonan et al.* 2002b], improve upon the data used by *Guenther et al.* [1995].

[19] CLM's global isoprene emission is similar to previous estimates and not lower, due to an offsetting process. CLM operates on a 20-min time step, while the same emission algorithms were driven with monthly average temperature in the work of *Guenther et al.* [1995]. CLM's higher time resolution can lead to emission increases [*Penner et al.*, 2001] for isoprene in particular, because isoprene originates mostly from broadleaf forests in warm temperatures. The temperature dependence of emissions is steeper the warmer the temperature, and the steeper the temperature dependence, the larger the effect of the shorter time step.

[20] Field measurements of isoprene fluxes have been made from various vegetation types around the world, and they indicate that our simulated emissions lie within the right order of magnitude (Figure 1). *Greenberg et al.* [1999] measured November/December late-morning isoprene fluxes of 3930 μg C m^{-2} hr^{-1} from tropical rain forest and 2520 μg C m^{-2} hr^{-1} from degraded woodland in Central Africa. *Pattey et al.* [1999] measured average daytime July isoprene fluxes of 2290 μg C m^{-2} hr^{-1} over a Canadian boreal forest. *Guenther et al.* [1996] estimated standardized isoprene fluxes on the order of 3000–4000 μg C m^{-2} hr^{-1} at two forested sites in southeastern United States. Rough agreement of our simulated emissions with these observations is satisfactory, because the meteorological and land use data used by the model at 1° by 1° resolution does not match the data at the specific times and sites that measurements were taken. Also, measurements made only during daylight hours will differ from (and be greater than) monthly average model output, which includes the full diurnal cycle.

[21] In a similar, but North America only simulation, we used natural vegetation where the satellite data include crops. We found that BVOC emissions increase significantly due to the higher LAI and emission capacities corresponding

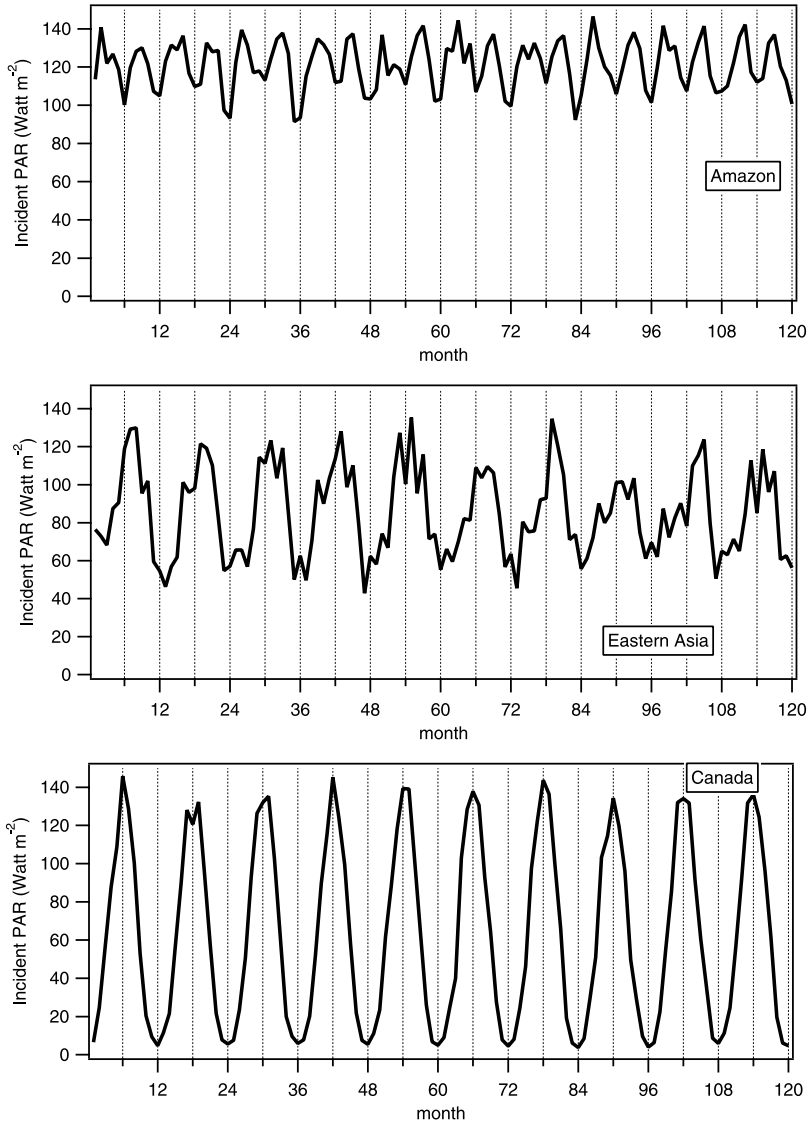

Figure 4. Simulated monthly incident PAR at the three grid cells illustrated in Figure 2.

to natural vegetation (Table 2). Greatest emission increases were found in the eastern half of North America and especially during the summer months (not shown). This result is consistent with previous studies showing the effects of land use on BVOC emissions [*Guenther et al.*, 1999; *Schaab et al.*, 2000].

3.2. CCSM Simulation

[22] Ten years of output from a CCSM simulation (atmosphere, ocean, sea ice, and land components all active) are analyzed. The land component, CLM, operates in dynamic vegetation mode. Human land use is not accounted for in this mode. The atmospheric component does not include chemistry and transport of emitted compounds at this time. Here we address interannual variability in the simulated BVOC emissions in response to variability in CCSM's simulated climate and vegetation.

[23] Annual simulated BVOC emissions vary by as much as 5% and monthly simulated emissions by as much as 18% from year to year over all land. These are comparable to values shown by *Naik et al.* [2002]. Three individual grid cells are selected to illustrate the behavior of interannual variability in these emissions: a tropical forest in Amazonia (grid center at 63.75°W, 1.86°S), a temperate deciduous forest in eastern Asia (grid center at 116.25°E, 31.54°N), and a boreal forest in Canada (grid center at 75.00°W, 57.52°N). Monthly terrestrial BVOC emissions are shown for the 10 simulation years (Figure 2).

[24] The emissions vary in response to changes in climate and LAI (Figures 3 and 4). In general, higher LAI, PAR, and temperature contribute to higher BVOC emissions. As a result, the tropical grid cell has higher BVOC emissions than the extra-tropical grid cells year-round. Interannual variability is more during the wet season (January through April). Monthly isoprene emissions vary by as much as 1.4 Tg C $month^{-1}$ in April from year to year, or approximately a factor of 2.5 (not shown). Monthly BVOC emissions vary by up to a factor of 2 and annual emissions by up to 29% from year to year. Simulated emissions integrated over the Amazon basin agree with the emissions reported by *Guenther* [2002] (near 0.2 Pg C yr^{-1}). The 10-year average basin-wide interannual variability is 4% in

CCSM compared to 10% simulated by *Guenther* [2002] in a 14-year simulation that accounts for the long-term variability in temperature.

[25] The boreal and temperate grid cells both show a seasonal pattern with maximum emissions during boreal summer. BVOC emissions from these grid cells are smaller than from the tropical grid cell, but the relative variations in the emissions tend to be larger. In particular, summer emissions of isoprene at both sites vary by as much as a factor of 3 from one year to another. Winter emissions are relatively small. Still, interannual variability is high, especially for January, mainly due to the high variability in winter temperature (Figure 3).

[26] Maximum LAI at the temperate grid cell doubles over the course of the ten years shown, as part of a regional trend caused by interannual variability in simulated climate and vegetation. BVOC emissions increase with time in response to the LAI. This grid cell consists mainly of broadleaf deciduous trees, which are strong isoprene emitters. As a result, this grid cell is highly sensitive to the variability in PAR (Figure 4).

4. Summary and Conclusions

[27] A terrestrial BVOC emissions module has been added to the CLM as one step toward introducing biogeochemical processes in the CCSM. CLM-simulated BVOC emissions and their spatial and temporal patterns generally agree with past modeling estimates. Emissions are sensitive to the choice of land cover, so it is advisable to include human land use when estimating BVOC emissions.

[28] In a fully coupled CCSM simulation (all model components active), the interannual variability in BVOC emissions is assessed. Global and point BVOC emissions vary substantially from year to year due to the simulated variability in climate and vegetation and play a role in the net ecosystem flux of carbon. *Tian et al.* [1998] investigated the interannual variability of CO_2 flux from the Amazon basin from 1981 to 1994 and found that the net ecosystem production varied from 0.7 Pg C yr^{-1} (a net uptake) to -0.2 Pg C yr^{-1} (a net release of CO_2). CCSM's simulated variability in BVOC emissions from the Amazon basin is of comparable magnitude.

[29] The IPCC estimates about 140 Tg C yr^{-1} of VOC emitted to the atmosphere from anthropogenic sources for the mid-1990s, and from less than 100 to more than 550 Tg C yr^{-1} for 2100 [*Nakicenovic et al.*, 2000]. The variability in global BVOC emissions shown in CCSM can exceed 10% of these estimated anthropogenic VOC emissions, suggesting an additional level of uncertainty in the emission scenarios that has not been accounted for. By introducing a model of BVOC emissions to the CCSM, our goal is to reduce climate uncertainty due to natural processes.

[30] The simulated interannual variability of BVOC emissions found at three sample grid cells also has local to regional implications. Emission changes can affect regional photochemistry. For example, ozone productivity could become NO_x-limited as opposed to VOC-limited in years when emissions are elevated, with repercussions on air quality. With the introduction of atmospheric chemistry and transport, as well as with a closed carbon cycle in the CCSM, we will be able to better understand the full range of effects of BVOC emissions and their variability.

[31] In this first attempt at simulating BVOC emissions in the CCSM we recognize some shortcomings. The plant functional types used in CLM are the same types that can be sensed by satellite and simulated by dynamic vegetation models. BVOC emission capacities (Table 2) are not easily categorized using the same list of plant functional types. For example, large amounts of isoprene are emitted from mosses and ferns [*Sharkey and Yeh*, 2001], which are not represented in CLM. Future studies may include region-specific emission capacities and plant types grouped according to alternate criteria. For the present study, the list of plant functional types is kept unchanged.

[32] The BVOC emissions model in CLM can be updated with more process-based algorithms. CLM calculates photosynthesis and stomatal conductance at every time step. Emissions of certain BVOC are linked to such plant physiological processes [*Guenther et al.* 2000], but these links have not, yet, been parameterized in global models.

[33] **Acknowledgments.** We thank two anonymous reviewers for their helpful comments. The National Center for Atmospheric Research is sponsored by the National Science Foundation.

References

Andreae, M. O., and P. J. Crutzen, Atmospheric aerosols: Biogeochemical sources and role in atmospheric chemistry, *Science*, *276*, 1052–1058, 1997.

Blackmon, M., et al., The Community Climate System Model, *Bull. Am. Meteorol. Soc.*, *82*, 2357–2376, 2001.

Bonan, G. B., A land surface model (LSM version 1.0) for ecological, hydrological, and atmospheric studies: Technical description and user's guide, *NCAR Tech. Note NCAR/TN-417+STR*, Natl. Cent. for Atmos. Res., Boulder, Colo., 1996.

Bonan, G. B., K. W. Oleson, M. Vertenstein, S. Levis, X. Zeng, Y. Dai, R. E. Dickinson, and Z.-L. Yang, The land surface climatology of the Community Land Model coupled to the NCAR Community Climate Model, *J. Clim.*, *15*, 3123–3149, 2002a.

Bonan, G. B., S. Levis, L. Kergoat, and K. W. Oleson, Landscapes as patches of plant functional types: An integrating concept for climate and ecosystem models, *Global Biogeochem. Cycles*, *16*(2), 1021, doi:10.1029/2000GB001360, 2002b.

Bonan, G. B., S. Levis, S. Sitch, M. Vertenstein, and K. W. Oleson, A dynamic global vegetation model for use with climate models: Concepts and description of simulated vegetation dynamics, *Global Change Biol.*, in press, 2003.

Bouchet, V. S., R. Laprise, E. Torlaschi, and J. C. McConnell, Studying ozone climatology with a regional climate model: 1. Model description and evaluation, *J. Geophys. Res.*, *104*, 30,351–30,371, 1999.

Collins, W. J., R. G. Derwent, C. E. Johnson, and D. S. Stevenson, The oxidation of organic compounds in the troposphere and their global warming potentials, *Clim. Change*, *52*, 453–479, 2002.

Constable, J. V. H., A. B. Guenther, D. S. Schimel, and R. K. Monson, Modeling changes in VOC emission in response to climate change in the continental United States, *Global Change Biol.*, *5*(7), 791–806, 1999.

Fehsenfeld, F., et al., Emissions of volatile organic compounds from vegetation and the implications for atmospheric chemistry, *Global Biogeochem. Cycles*, *6*, 389–430, 1992.

Foley, J. A., S. Levis, M. H. Costa, W. Cramer, and D. Pollard, Incorporating dynamic vegetation cover within global climate models, *Ecol. Appl.*, *10*, 1620–1632, 2000.

Greenberg, J. P., A. Guenther, S. Madronich, W. Baugh, P. Ginoux, A. Druilhet, R. Delmas, and C. Delon, Biogenic volatile organic compound emissions in central Africa during the Experiment for the Regional Sources and Sinks of Oxidants (EXPRESSO) biomass burning season, *J. Geophys. Res.*, *104*, 30,659–30,671, 1999.

Griffin, R. J., D. R. Cocker III, and J. H. Seinfeld, Estimate of global atmospheric organic aerosol from oxidation of biogenic hydrocarbons, *Geophys. Res. Lett.*, *26*(17), 2721–2724, 1999.

Guenther, A., The contribution of reactive carbon emissions from vegetation to the carbon balance of the terrestrial ecosystem, *Chemosphere*, *49*, 837–844, 2002.

Guenther, A., P. R. Zimmerman, P. C. Harley, R. K. Monson, and R. Fall, Isoprene and monoterpene emission rate variability: Model evaluations and sensitivity analyses, *J. Geophys. Res.*, *98*, 12,609–12,617, 1993.

Guenther, A., P. Zimmerman, and M. Wildermuth, Natural volatile organic compound emission rate estimates for U.S. woodland landscapes, *Atmos. Environ.*, *28*, 1197–1210, 1994.

Guenther, A., et al., A global model of natural volatile organic compound emissions, *J. Geophys. Res.*, *100*, 8873–8892, 1995.

Guenther, A., et al., Estimates of regional natural volatile organic compound fluxes from enclosure and ambient measurements, *J. Geophys. Res.*, *101*, 1345–1359, 1996.

Guenther, A., et al., Biogenic hydrocarbon emissions and landcover/climate change in a subtropical savanna, *Phys. Chem. Earth, Part B, Hydrol. Oceans Atmos.*, *24*, 659–667, 1999.

Guenther, A., C. Geron, T. Pierce, B. Lamb, P. Harley, and R. Fall, Natural emissions of non-methane volatile organic compounds, carbon monoxide, and oxides of nitrogen from North America, *Atmos. Environ.*, *34*, 2205–2230, 2000.

Houweling, S., F. Dentener, and J. Lelieveld, The impact of nonmethane hydrocarbon compounds on tropospheric chemistry, *J. Geophys. Res.*, *103*, 10,673–10,696, 1998.

Kalnay, E., et al., The NCEP/NCAR 40-year reanalysis project, *Bull. Am. Meteorol. Soc.*, *77*, 437–471, 1996.

Kucharik, C. J., et al., Testing the performance of a dynamic global ecosystem model: Water balance, carbon balance, and vegetation structure, *Global Biogeochem. Cycles*, *14*, 795–825, 2000.

Liousse, C., J. E. Penner, C. Chuang, J. J. Walton, H. Eddleman, and H. Cachier, A global three-dimensional model study of carbonaceous aerosols, *J. Geophys. Res.*, *101*, 19,411–19,432, 1996.

Naik, V., C. Delire, and D. J. Wuebbles, Modeling the climate variability of biogenic isoprene and monoterpenes, *Eos Trans. AGU*, *83*(47), Fall Meet. Suppl., Abstract A61B-0076, 2002.

Nakicenovic, N., et al., *Emissions Scenarios: A Special Report of Working Group III of the Intergovernmental Panel on Climate Change*, edited by N. Nakicenovic and R. Swart, 612 pp., Cambridge Univ. Press, New York, 2000.

Pattey, E., R. L. Desjardins, H. Westberg, B. Lamb, and T. Zhu, Measurement of isoprene emissions over a black spruce stand using a tower-based relaxed eddy-accumulation system, *J. Appl. Meteorol.*, *38*, 870–877, 1999.

Penner, J. E., et al., Aerosols, their direct and indirect effects, in *Climate Change 2001: The Scientific Basis: Contribution of Working Group I to the Third Assessment Report of the Intergovernmental Panel on Climate Change*, edited by J. T. Houghton et al., pp. 289–348, Cambridge Univ. Press, New York, 2001.

Penuelas, J., and J. Llusia, The complexity of factors driving volatile organic compounds emissions by plants, *Biol. Plantarum*, *44*(4), 481–487, 2001.

Pierce, T., C. Geron, L. Bender, R. Dennis, G. Tonnesen, and A. Guenther, The influence of increased isoprene emissions on regional ozone modeling, *J. Geophys. Res.*, *103*, 25,611–25,629, 1998.

Poisson, N., M. Kanakidou, and P. J. Crutzen, Impact of non-methane hydrocarbons on tropospheric chemistry and the oxidizing power of the global troposphere: 3-dimensional modeling results, *J. Atmos. Chem.*, *36*, 157–230, 2000.

Potter, C. S., S. E. Alexander, J. C. Coughlan, and S. A. Klooster, Modeling biogenic emissions of isoprene: Exploration of model drivers, climate control algorithms, and use of global satellite observations, *Atmos. Environ.*, *35*, 6151–6165, 2001.

Running, S. W., T. R. Loveland, L. L. Pierce, R. R. Nemani, and E. R. Hunt Jr., A remote sensing based vegetation classification logic for global land cover analysis, *Remote Sens. Environ.*, *51*, 39–48, 1995.

Schaab, G., R. Steinbrecher, B. Lacaze, and R. Lenz, Assessment of long-term changes on potential isoprenoid emissions for a Mediterranean type ecosystem in France, *J. Geophys. Res.*, *105*, 28,863–28,874, 2000.

Sharkey, T. D., and S. S. Yeh, Isoprene emission from plants, *Annu. Rev. Plant Phys.*, *52*, 407–436, 2001.

Sitch, S., et al., Evaluation of ecosystem dynamics, plant geography and terrestrial carbon cycling in the LPJ dynamic global vegetation model, *Global Change Biol.*, *9*, 161–185, 2003.

Tian, H., J. Melillo, D. Kicklighter, A. D. McGuire, J. Helfrich III, B. Moore III, and C. Vorosmarty, Effect of interannual climate variability in Amazonian ecosystems, *Nature*, *396*, 664–667, 1998.

Wang, K. Y., and D. E. Shallcross, Modelling terrestrial biogenic isoprene fluxes and their potential impact on global chemical species using a coupled LSM-CTM model, *Atmos. Environ.*, *34*, 2909–2925, 2000.

G. B. Bonan, A. Guenther, S. Levis, and C. Wiedinmyer, National Center for Atmospheric Research, PO Box 3000, Boulder, CO 80307-3000, USA. (slevis@ucar.edu)